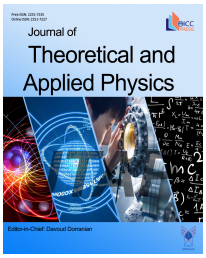

Volume 18, Issue 5, 182464 (1-14)

Journal of Theoretical and Applied Physics (JTAP)

https://dx.doi.org/10.57647/j.jtap.2024.1805.64

High-sensitivity detection of SARS-CoV-2 using optimized carbon nanotube field-effect transistor (CNTFET) geometry: a numerical approach

Oussama Zeggai[1,2], Mousaab Belarbi[3,*], Abdesslam Bouhenna[4], Sami Khettaf[5], Hadj Mouloudj[1], Amaria Ouledabbes[2]

[1]*Department of Common Core, Faculty of Exact Sciences and Informatics, Hassiba Ben Bouali University, Chlef, Algeria.*
[2]*Research Unit Materials and Renewable Energy (URMER), Abou Bekr Belkaïd University, Tlemcen, Algeria.*
[3]*Laboratory of Micro and Nanophysics-LaMiN, Department of FPST-Ecole Nationale Polytechnique d'Oran-Maurice Audin, Oran, Algeria.*
[4]*Laboratory for Theoretical Physics and Material Physics, Department of Physics, Faculty of Exact Sciences and Informatics, Hassiba Benbouali University of Chlef, Algeria.*
[5]*Laboratory of Chemistry and Environmental Chemistry LCEE, Department of Chemistry, Faculty of Material Sciences, University of Batna, Batna, Algeria.*

[*]**Corresponding author:** moussaab.belarbi@enp-oran.dz

Original Research

Received:
1 August 2024
Revised:
6 September 2024
Accepted:
12 September 2024
Published online:
30 October 2024

Abstract:

This study presents a comprehensive numerical analysis of carbon nanotube (CNT)-based field-effect transistor (FET) sensors designed to detect SARS-CoV-2, the virus responsible for COVID-19. While graphene-based FETs have been extensively studied, our research emphasizes the unique advantages of CNTs, including enhanced sensitivity and seamless integration into existing technologies. Through numerical simulations, we evaluated the influence of CNT geometry, specifically length and diameter, on FET sensor performance. The results demonstrate that optimized CNT geometries significantly enhance sensor sensitivity and accuracy, providing superior capabilities for the rapid and precise detection of SARS-CoV-2. These findings underscore the potential for developing reliable, fast, and cost-effective CNT-based FET biosensors for effective pandemic response and broader public health applications.

Keywords: Carbon nanotube field-effect transistor (CNTFET); SARS-CoV-2 detection; High-sensitivity biosensors; Numerical optimization

1. Introduction

The outbreak of COVID-19, caused by the novel SARS-CoV-2 virus, first identified in Wuhan, Hubei province, China, in December 2019, rapidly escalated into a global pandemic [1]. This virus has led to significant human suffering and economic disruption worldwide. As of early 2021, it has resulted in millions of infections and fatalities, underscoring the critical need for rapid, effective, and widespread testing and diagnostic methods [2]. While traditional diagnostic methods such as polymerase chain reaction (PCR) and enzyme-linked immunosorbent assay (ELISA) are reliable, they often require substantial time and resources, highlighting the necessity for innovative approaches that can provide faster results with high accuracy and minimal resource consumption [3, 4].

In recent years, carbon nanotubes (CNTs) have emerged as one of the most promising nanomaterials, thanks to their unique combination of exceptional electrical conductivity, chemical stability, and mechanical strength [5]. These properties make CNTs particularly well-suited for biosensing applications, especially in field-effect transistor (FET) sen-

sors, which have shown great potential in detecting a wide range of analytes, including viruses, due to their high sensitivity and rapid response times [6–10].

Field-effect transistor (FET)-based biosensors operate by detecting changes in electrical conductivity in response to the binding of target analytes. Carbon nanotubes, acting as the conducting channel in these sensors, can be functionalized with specific biomolecules, such as antibodies, to selectively detect the presence of corresponding antigens, including the spike proteins of viruses like SARS-CoV-2 [11]. The versatility and sensitivity of these CNT-based FET biosensors make them a promising tool for detecting a wide range of biological targets, as highlighted in several recent studies, including their use in the detection of critical biomarkers such as C-reactive protein (CRP) for cardiovascular disease and myoglobin for acute myocardial infarction [12, 13]. Several recent studies have explored the broader potential of nanomaterial-based biosensors, including CNT-FETs, in the rapid and sensitive detection of pathogens, particularly during pandemics.

For instance, William Reis de Araujo et al. (2024) emphasized the importance of frequent point-of-care testing for controlling outbreaks, focusing on nanomaterial-based optical and electrochemical biosensors. They compared these to conventional methods such as PCR, ELISA, and loop-mediated isothermal amplification (LAMP), discussing their advantages and challenges. The study underscored how these nanobiosensors could be crucial in managing future pandemics [14]. Similarly, Ruiqi Wang et al. (2024) highlighted the limitations of PCR-based methods and the need for new detection techniques for SARS-CoV-2. Their work stressed the importance of early warning systems and sensitive diagnostics, facilitated by a better understanding of viral protein structures, to improve outbreak response [15].

Further advancing this field, Yuqi Liang et al. (2023) developed a multi-functionalized floating gate carbon nanotube field-effect transistor (FG-CNT FET) biosensor capable of rapidly and sensitively detecting SARS-CoV-2 antigens and ribonucleic acid (RNA). This portable sensor can detect viral antigens from unprocessed nasopharyngeal swab samples within one minute and directly detect RNA without amplification at the single-virus level. Clinical tests accurately distinguished COVID-19 patients and healthy individuals, highlighting its potential for point-of-care clinical testing [16].

Moreover, Farzaneh Mirzadeh-Rafie et al. (2023) discussed the need for rapid, cost-effective COVID-19 diagnostics beyond early methods like computed tomography (CT) scans and PCR. They explored using carbon-based nanobiosensors for real-time virus detection, noting their exceptional properties and effectiveness. The study introduced various nano-biosensors with different detection limits, emphasizing their potential to control the spread of COVID-19 [17]. Similarly, M. Thanihaichelvan et al. (2022) proposed a CNT FET-based biosensor for the selective detection of SARS-CoV-2. Their CNT FETs, fabricated on a flexible Kapton substrate, demonstrated a selective response to the target sequence with a detection limit of 10 femtomolar (fM), indicating the potential of CNT FET-based biosensors as practical diagnostic tools for SARS-CoV-2 detection [18].

Despite these advancements, the specific application of CNT-FETs for detecting SARS-CoV-2 has yet to be exhaustively explored, particularly regarding optimizing the physical parameters of the CNTs, such as length, diameter, and chirality. These structural properties critically influence the interaction between CNTs and virus particles, affecting overall sensor performance.

This study aims to bridge this gap by providing a detailed numerical simulation of the interactions between SARS-CoV-2 and CNT-based FETs. By modeling the changes in the electronic properties of CNTs upon binding with the virus, we seek to understand how various configurations of CNT geometry can enhance detection capabilities. This research not only contributes to the scientific understanding of nanomaterial-based biosensors but also paves the way for the development of more efficient, rapid, and cost-effective diagnostic tools that are urgently needed to combat ongoing and future pandemics.

Our findings are expected to offer significant insights into the optimal design of CNT-based FET biosensors, thereby contributing to the development of more sensitive and selective biosensors for the rapid and accurate detection of SARS-CoV-2. Such advancements could profoundly impact public health, enhancing our ability to respond swiftly and effectively to pandemic threats.

The following sections provide an overview of the SARS-CoV-2 virus (Section 2), detail the materials and methods used in this study (Section 3), which includes the structural properties of CNTs (Section 3.1), the modeling of CNTFETs (Section 3.2), their application in SARS-CoV-2 detection (Section 3.3), and the simulation and numerical analysis (Section 3.4). The results and discussion are presented in Section 4, followed by the conclusion in Section 5.

2. The SARS-CoV-2 virus

The rapid increase in confirmed SARS-CoV-2 cases has been relentless, with approximately 200,000 new cases diagnosed daily worldwide as of early 2021. According to official data from the world health organization (WHO), this global pandemic has resulted in over 1,700,000 infections and more than 670,000 deaths [19]. SARS-CoV-2, the virus responsible for the COVID-19 disease [20], was named for its genetic similarity to the severe acute respiratory syndrome coronavirus 1 (SARS-CoV-1), first identified in 2003. Early symptoms of COVID-19 include fever, dry cough, shortness of breath, headaches, muscle pain, and fatigue [21]. However, these symptoms are not definitive, as asymptomatic carriers of SARS-CoV-2 have been identified, and symptoms overlap with other acute respiratory viral infections such as influenza [22].

SARS-CoV-2 belongs to a family of RNA viruses that infect various vertebrate animals. These viruses are named for their crown-like (corona) envelope, composed of a lipid membrane with spike-shaped proteins embedded within it (Figure 1). While most commonly found in bats, coronaviruses can infect other mammals, such as humans, whales, and birds. In humans, coronaviruses typically cause mild

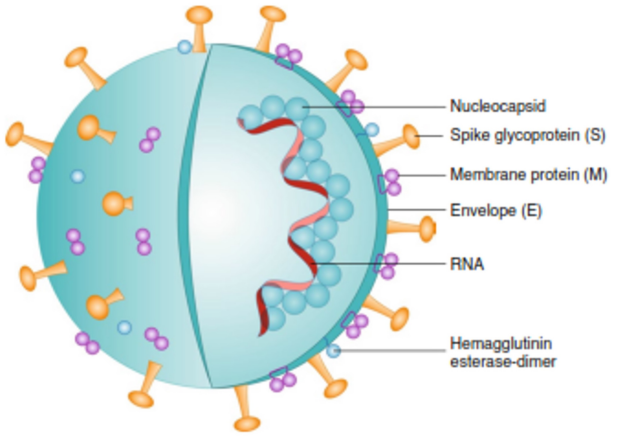

Figure 1. Schematic representation of the SARS-CoV-2 virus.

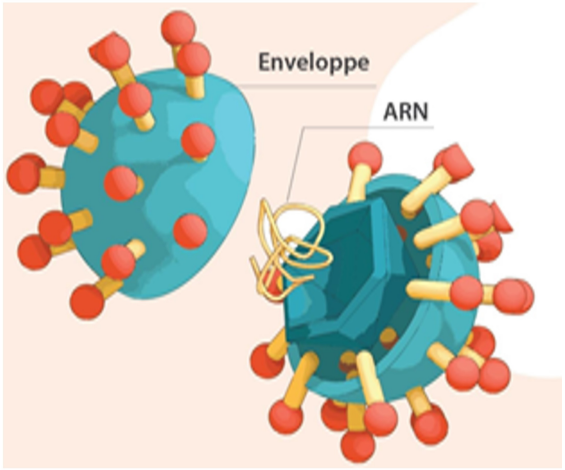

Figure 2. SARS-CoV-2 RNA structure.

respiratory tract infections like the common cold; however, they can also lead to severe respiratory distress, resulting in complications and potentially fatal outcomes in some cases [23].

With an average diameter of 80 nanometers (nm), SARS-CoV-2 is invisible to the naked eye, being approximately 300 times thinner than a strand of hair. Like all coronaviruses, SARS-CoV-2 is an enveloped virus with a single-stranded RNA genome. This RNA encodes the synthesis of four structural proteins (Figure 2) and 16 non-structural proteins involved in viral replication [24, 25]. The four structural proteins include the *S* (spike), *E* (envelope), *M* (membrane), and *N* (nucleocapsid) proteins (Figure 1). The spike protein binds the virus to the ACE2 receptor on the human host cell's membrane surface, facilitating entry and infection [26, 27]. Thus, the spike acts as the key that attaches to the lock (ACE2 protein), allowing the virus to enter cells expressing this receptor [28].

Carbon nanotubes (CNTs) have been extensively used in the development of biosensors, primarily focusing on electrochemical [29, 30], optical [31, 32], and field-effect [33, 34] devices. To fully harness the exceptional properties of this nanomaterial in biosensor creation, CNTs need to be purified and functionalized with biorecognition elements. Designing the biological sensing interface is a critical challenge in biosensor development, as both functionalization and transduction steps must be considered. Effective immobilization of the biorecognition element is crucial for selective recognition of the analyte on the biosensor's surface. Additionally, the transduction mechanism must be optimized to swiftly and sensitively detect minor changes in the biorecognition element resulting from the presence of the target analyte.

3. Materials and methods

3.1 Structure and properties of carbon nanotubes (CNTs)

Carbon nanotubes (CNTs) are continuous, hollow cylinders formed from rolled graphite layers. Based on the number of graphite layers, CNTs can be categorized into single-walled carbon nanotubes (SWCNTs) and multi-walled carbon nanotubes (MWCNTs) [35, 36], as depicted in Figures 3 (a) and 3 (b), respectively. Generally, SWCNTs are single molecular nanomaterials formed by rolling a single graphene sheet into a seamless molecular cylinder. Their diameter and length typically range from 0.75 to 3 nm and 1 to 50 nm, respectively. In contrast, MWCNTs consist of two or more layers of rolled graphite sheets, with diameters ranging from 2 to 30 nm and sometimes exceeding 100 nm (Figure3 (b)) [37]. The distance between each layer is approximately 0.42 nm.

Single-walled carbon nanotubes (SWCNTs) have the most straightforward morphology and can be envisioned as a single rolled-up graphene sheet. A nanotube's structure can be easily defined through its chiral vector, which is based on the tube axis's orientation relative to the hexagonal lattice. The chiral vector is represented by Equation (1) and is determined by the chiral indices (n, m), as shown in Figure 4.

$$\mathbf{C}_h = n\mathbf{a}_1 + m\mathbf{a}_2 \tag{1}$$

where ($\mathbf{C}$) a linear combination of the lattice basis vectors ($\mathbf{a}_1$) and ($\mathbf{a}_2$); n and m are positive integers called chiral indices [39, 40].

According to different winding directions, SWCNTs are divided into three structural types: armchair, zigzag and chiral [41]. The structural type of CNTs is related to their chiral vector (n, m) and the chiral angle θ. As shown in Figure 4 [38], when $n = m$, the chiral angle is equal to 30° between the chiral vector ($\mathbf{C}_h$) and the lattice vector ($\mathbf{a}_1$); this type of CNT is called armchair. When $m = 0$, $\theta = 0°$, the type of CNT is called zigzag. When $n \neq m$ and $0 < \theta < 30°$, the CNT type is said to be chiral. The dependence on the chiral vector and angle determines the electronic structure of the CNTs, resulting in either semiconductor or metallic properties.

Based on chirality, the diameter of a single-walled nanotube is given by the following equation:

$$D_{\mathrm{CNT}} = \frac{a}{\pi}\sqrt{n^2 + m^2 + nm} \tag{2}$$

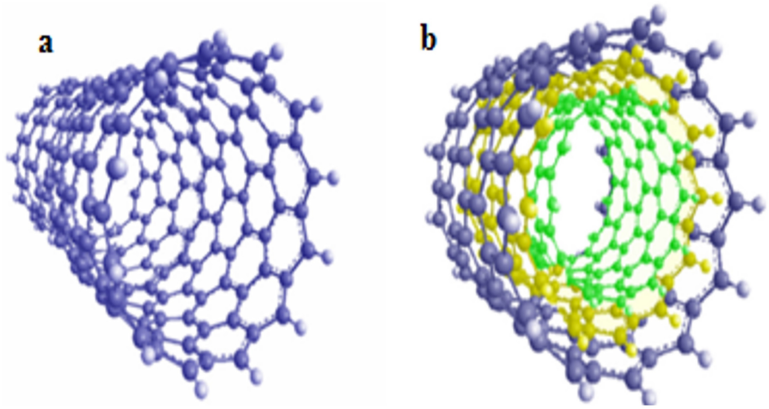

Figure 3. Structure of (a) a single-walled carbon nanotube (SWCNT) and (b) a multi-walled carbon nanotube (MWCNT).

where $a = 0.142$ nm is the lattice constant of graphene. The following equation gives the nanotube length:

$$L = a\sqrt{n^2 + m^2 + nm} \tag{3}$$

The chiral angle θ, also called helicity, is obtained by the following relationship:

$$\theta = \arctan\frac{\sqrt{3}m}{m + 2m} \tag{4}$$

For CNT lengths shorter than the mean free path, electron transport is ballistic within the nanotube, and the resistance is independent of the length [42, 43]. However, for lengths greater than the mean free path, the resistance increases with length as:

$$R = (\frac{h}{4e^2})\frac{L}{L_0} \tag{5}$$

where h is Planck's constant, e is the charge of an electron, L is the length of the CNT, L_0 is the mean free path (1000 nm).

The electrostatic capacitance of a CNT is calculated by treating the CNT as a thin wire of diameter d, placed at a distance y from a ground plane, and is given by:

$$C_E = \frac{2\pi\varepsilon}{\ln\frac{y}{d}} \tag{6}$$

where ε is the permeability ($\varepsilon = \varepsilon_0 \cdot \varepsilon_r$, $\varepsilon_0 = 4\pi \times 10^{-7}$, $\varepsilon_r = 2$).

Carbon nanotubes (CNTs) have emerged as one of the most extensively utilized nanomaterials. As research in this dynamic field advances, various forms of CNTs are being modeled and produced, garnering significant attention across numerous domains. One notable area of interest is the application of CNTs in biosensors. Their unique structure and nanoscale dimensions grant CNTs numerous advantageous properties for chemical and biological sensing applications, including large surface-to-electrolyte ratios, outstanding electrical conductivities, high chemical stability, and fluorescence capabilities.

3.2 Modeling of carbon nanotube field-effect transistors (CNTFETs)

The device examined in this simulation is a carbon nanotube field-effect transistor (CNTFET) of the metal-oxide-semiconductor field-effect transistor (MOSFET) type. In this structure, the drain and source terminals are heavily doped. The device's operating principle relies on barrier height modulation through the application of gate voltage, which causes the drain current to depend on the number of charges induced in the channel by the gate voltage. Figure 5 displays the top view of the carbon nanotube field-effect transistor.

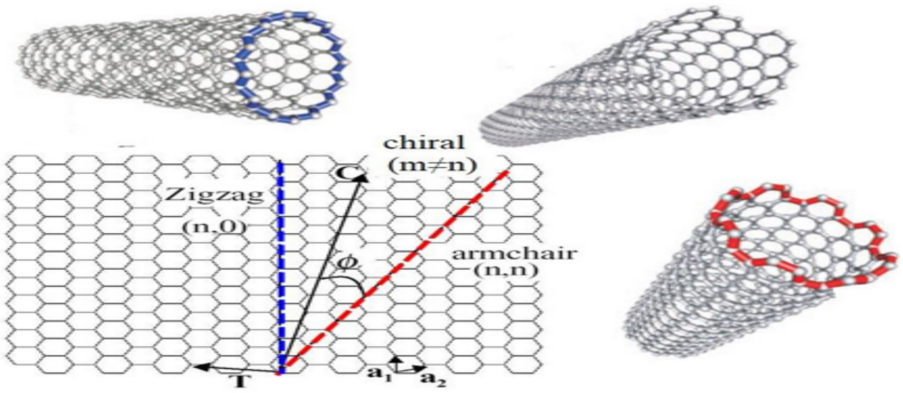

Figure 4. Construction of a carbon nanotube from a single sheet of graphene. The chiral vector determines different types of nanotubes [38].

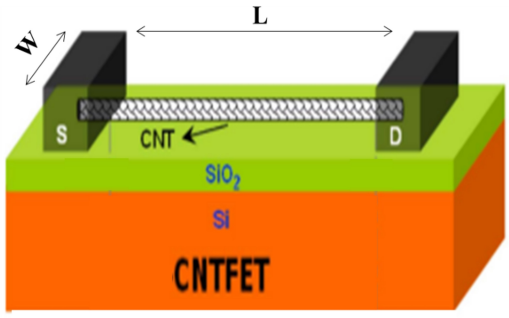

Figure 5. Structure of the carbon nanotube field-effect transistor.

The primary design parameters for the CNTFET include the number of CNTs in a transistor (N), the inter-CNT gap (S), and the carbon nanotube diameter (DCNT) [44]. The gate's length and width are denoted by Lgate and Wgate, respectively. The threshold voltage (V_{th}), CNTFET base transistor width (W), number of CNTs in the channel (N), inter-CNT spacing (S), and energy gap (E_g) are related through Equations (7) to (9):

$$V_{th} = \frac{aV_\pi}{qD_{\text{CNT}}} \tag{7}$$

$$W = (N-1)\cdot S + D_{\text{CNT}} \tag{8}$$

$$E_g = \frac{0.84\ (\text{eV})}{D_{\text{CNT}}} \tag{9}$$

where q is the electronic charge and $V_\pi = 3.033$ eV is the carbon $\pi - \pi$ bond energy.

The current equation is derived under the assumption of ballistic transport in the CNT, enabling the electric current calculation. The drain current of the transistor is represented by Equation (10) [45]:

$$I_D = \frac{4qKT}{h}[\ln(1+\exp(\xi_s)) - \ln(1+\exp(\xi_D))] \tag{10}$$

where

$$\xi_s = \frac{\emptyset_s - \delta_1}{V_T} \tag{11}$$

$$\xi_D = \frac{\emptyset_s - \delta_1 - V_{DS}}{V_T} \tag{12}$$

$$\emptyset_s = \frac{V_{GS} - qn}{C_{ox}} \tag{13}$$

In these equations, n is the carrier density in the channel, and δ_1 is the equilibrium subband minimum of the first subband ($E_g/2$). The constant terms q, k, h, and T represent the charge of the electron, Boltzmann constant, Planck constant, and absolute temperature, respectively, while V_{GS} and V_{DS} are the gate-source and drain-source voltages of the CNTFET model [46, 47].

Furthermore, the relationship between the nanotube diameter (D_{CNT}), oxide thickness (t_{ox}), and oxide capacitance (C_{ox}) of the CNTFET is given by Equation (14):

$$C_{ox} = \frac{2\pi\varepsilon_0\varepsilon_{ox}}{\ln(\frac{2t_{ox}}{D_{\text{CNT}}}) + 1} \tag{14}$$

The thermal stress relation is provided by Equation (15):

$$V_T = \frac{KT}{q} \tag{15}$$

These detailed relationships and equations form the basis of understanding the electrical behavior and performance of CNTFETs, which are crucial for optimizing their design and application in biosensors.

3.3 Application of carbon nanotube field-effect transistors (CNTFETs) in SARS-CoV-2 detection

Figure 6 presents the biosensor block diagram featuring a cell or molecule in an analyte. A biosensor is a bioanalytical device with two fundamental components: a bioreceptor and a signal transducer. The bioreceptor detects target analytes with specificity, while the transducer elements convert the biochemical event into a quantifiable signal. The output of the transduction element indicates the analyte concentration in a test sample of a biological solution [48, 49].

In this figure, various bioreceptor types such as antibodies, enzymes, cells, aptamers, and nanoparticles are depicted, each capable of specific interactions with the target analyte. These bioreceptors trigger a biochemical conversion that is then transduced into an electrical, optical, thermal, or mechanical signal, depending on the transducer mechanism employed.

Field-effect transistor (FET) technology, highlighted within the transducer component, offers a promising platform for rapidly and precisely detecting various analytes [50]. It has been successfully used to detect target analytes in gases [51, 52] and water [53, 54]. FET sensors boast advantages such as quick response, low cost, and ease of use, as real-time results can be monitored with affordable meters that can be calibrated for different applications [55]. By anchoring specific probes to the conductive channel, FET biosensors can achieve high sensitivity and selectivity for particular biomolecules [56, 57], which is critical for FET sensor performance.

One-dimensional semiconductor materials, like carbon nanotubes and zinc oxide nanowires, are especially appealing as conductive channels for FET biosensors due to their exceptional electronic properties. Carbon nanotubes (CNTs) have been utilized as conducting channels in FET biosensors for SARS-CoV-2 virus detection [58]. A carbon nanotube-based FET biosensor should have sensitivity

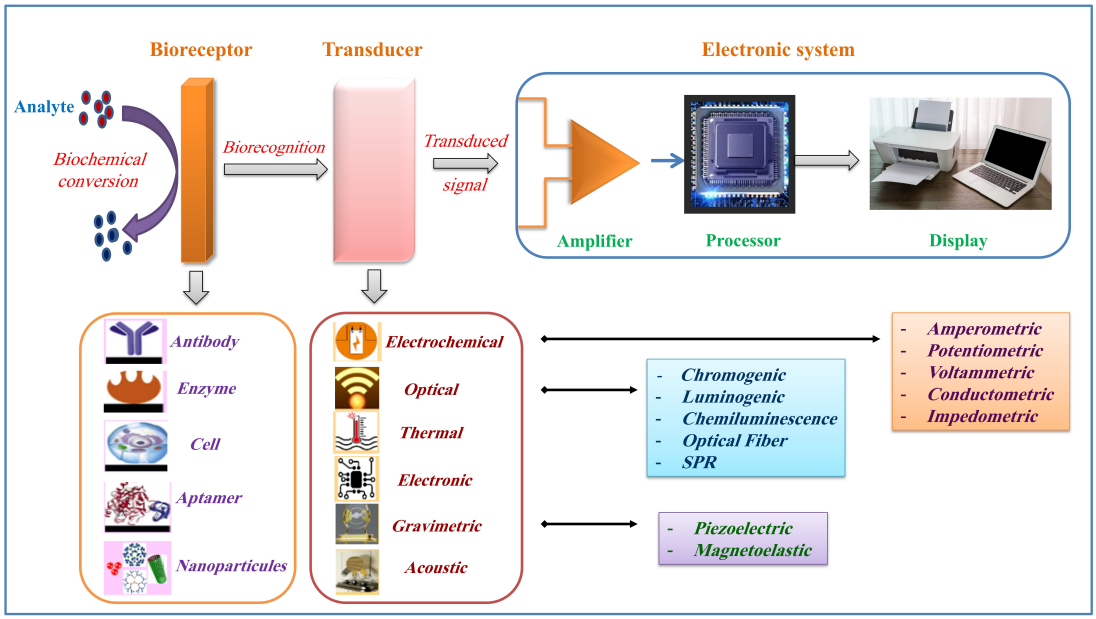

Figure 6. Schematic block diagram of the biosensor.

comparable to PCR, a lower cost per test, and minimal investment in required laboratory equipment.

Among the various viable identification techniques for detecting viral proteins, field-effect transistor (FET)-based biosensors offer benefits such as exceptional sensitivity, small dimensions, and label-free, real-time detection. Carbon nanotube-based FETs have recently been utilized for COVID-19 detection, and a label-free CNTFET immunosensor has been designed to recognize and capture the SARS-CoV-2 *S*1 spike protein [59]. Detection is based on the highly specific interaction between the SARS-CoV-2 spike *S*1 protein and the SARS-CoV-2 spike *S*1 subunit protein antibody or a functionalized carbon nanotube surface using human angiotensin-converting enzyme 2 (ACE2) [60]. The development of the SARS-CoV-2 viral detection platform incorporates a carbon nanotube-based FET biosensing device functionalized with a state-of-the-art anti-SARS-CoV-2 antibody. The CNTFET COVID-19 sensor identifies SARS-CoV-2 spike *S*1 proteins in nasopharyngeal swabs and can detect SARS-CoV-2 when RNA is present. Carbon nanotube-based FET sensors have shown potential for COVID-19 diagnosis applications, offering high sensitivity and reduced detection times [61].

To create the CNTFET element for COVID-19 detection (Figure 7), interdigitated gold electrodes were designed on a Si/SiO_2 substrate through photolithography, establishing 10 µm channels. Semiconductor SWCNTs (IsoSol-S100, Raymor Industries Inc.) were prepared at a concentration of 0.02 mg/mL in toluene and placed between gold electrodes using dielectrophoresis (DEP), with a 100 kHz alternating frequency, a 10 V applied voltage bias, and a 120 s bias duration. The devices underwent annealing at 200 °C for one hour prior to utilization.

The functionalization of the SARS-CoV-2 antibody on SWCNTs was accomplished using 1- ethyl-3-(3-dimethylaminopropyl) carbodiimide (EDC)/N-hydroxysulfosuccinimide (sulfo-NHS) coupling. Specifically, 50 µL of EDC/sulfo-NHS solution [50 mM/50 mM in 1× phosphate-buffered saline (PBS), pH = 5.5] was initially applied to the devices to activate the carboxylic

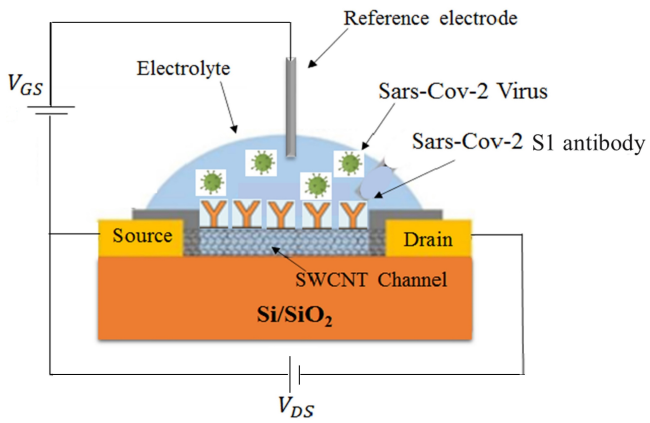

Figure 7. SWCNT-based FET biosensor for COVID-19 detection.

acid groups on SWCNTs. The devices were subsequently rinsed with nanopure water and incubated with 2 µL of 100 µg/mL polyclonal SARS/SARS-CoV-2 coronavirus spike protein (subunit 1) antibody (Thermo Fisher Scientific, Waltham, MA, USA; Cat# PA5-81795) for 12 hours at 4 °C for SAb-functionalized devices, and 4 µL of 50 µg/mL anti-SARS-CoV-2 NP antibody (clone # 6F10) (BioVision Inc., Milpitas, CA, USA; Cat# A2060) for NAb-functionalized devices. After thoroughly rinsing with nanopure water to ensure the removal of unbound reagents, the devices were immersed in a blocking buffer (0.1% Tween 20 and 4% polyethylene glycol in PBS) for 30 minutes to cover unreacted surfaces. Following the blocking step, the devices were rinsed again with nanopure water before performing any FET measurements [62, 63]. During virus detection, the antibodies exhibited strong signals, likely due to their ability to recognize the target molecule and the tighter binding that enhances detection sensitivity. The binding process of antigen-antibody complexes can be modeled by Langmuir's extended isotherm, which correlates sensor gain with antigen concentration [64]:

$$\Delta V = \frac{q_m b[c]^\eta}{1 + b[c]^\eta} \tag{16}$$

where q_m and b are constants, $[c]$ is the antigen concentration tested, and η relates to the spread of the energy distribution.

3.4 Simulation and numerical analysis

The simulation was performed in the MATLAB environment, considering various parameters such as length, diameter, and chirality angle, which represent the electrical properties of carbon nanotubes (CNTs). Additionally, the gate voltage variation in the CNTFET device was analyzed for different SARS-CoV-2 concentrations. Since SARS-CoV-2 is converted into negative charges through antibodies, our study focuses on how these electrical properties influence the electric current, with particular attention to the CNT's diameter, chirality angle, and length, alongside the concentration of SARS-CoV-2.

This study provides a comprehensive numerical analysis of CNTFETs for SARS-CoV-2 detection, emphasizing the critical role of CNT geometry in sensor performance. By exploring the interaction between SARS-CoV-2 and CNTs, we aim to optimize the design parameters for CNTFET biosensors, thereby enhancing their sensitivity and specificity. The detailed insights gained from this simulation are expected to significantly contribute to the development of more efficient, rapid, and cost-effective diagnostic tools for pandemic response.

4. Results and discussion

Building upon the CNT properties and modeling framework established in the previous sections, we now present the key findings from our study. These results illustrate the critical relationships between various CNT parameters and the performance of CNTFETs in the context of SARS-CoV-2 detection.

Figure 8 shows the relationship between the resistance of carbon nanotubes and their length. As depicted, there is a linear increase in resistance with the length of the CNTs, indicating ohmic conduction, where resistance is directly proportional to the conductor length. The graph demonstrates that for shorter CNT lengths, the resistance remains relatively low, which benefits applications requiring low-resistance pathways, such as interconnections in electronic devices and sensors.

In the context of CNTFET biosensors for SARS-CoV-2 detection, maintaining low resistance is crucial for ensuring high sensitivity and fast response times. The linear increase in resistance indicates that CNTs may become less effective beyond a certain length due to higher resistive losses. Therefore, optimizing the length of CNTs within the biosensor is essential to balance sensitivity and resistance, achieving maximum performance in detecting the virus.

Figure 9 illustrates the capacitance of carbon nanotubes as a function of their diameter. The capacitance increases exponentially with the diameter of the CNTs, attributed to the larger surface area of CNTs with greater diameters, enhancing their ability to store charge. A higher capacitance can

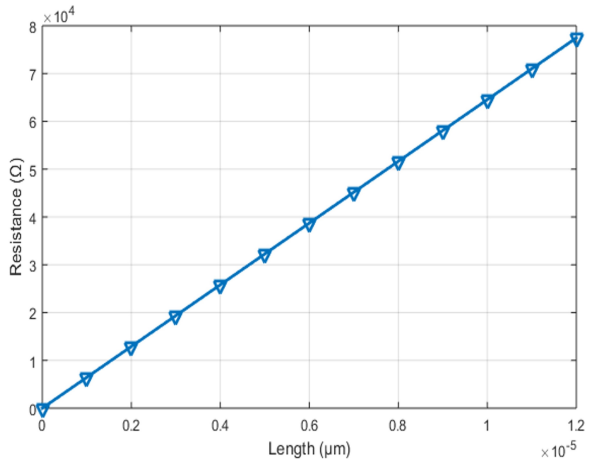

Figure 8. Resistance of carbon nanotubes as a function of length.

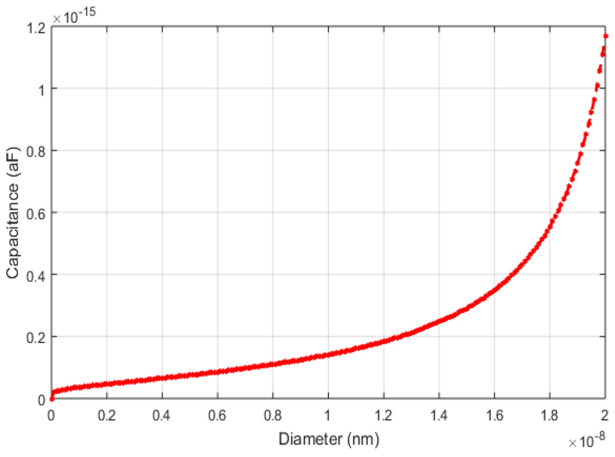

Figure 9. Capacitance of carbon nanotubes as a function of diameter.

enhance the sensor's sensitivity in biosensing applications by enabling more efficient interaction with target molecules. Higher capacitance is advantageous for CNTFET biosensors designed to detect SARS-CoV-2 because it improves the device's ability to transduce biological interactions into measurable electrical signals. The exponential increase with diameter underscores the importance of selecting CNTs with optimal diameters to maximize the sensor's sensitivity and overall performance. However, balancing this with other factors, such as ease of fabrication and the mechanical stability of larger-diameter CNTs, is essential.

These findings provide valuable insights into how the physical properties of CNTs, such as length and diameter, affect their electrical characteristics. These insights are crucial for optimizing the design parameters of CNTFET biosensors, ensuring they are highly sensitive, reliable, and effective in detecting SARS-CoV-2.

Figure 10 shows the relationship between the threshold voltage (V_{th}) of CNTFETs and the diameter of the carbon nanotubes. The graph indicates that the threshold voltage significantly decreases as the diameter increases. This inverse relationship is crucial because a lower threshold voltage enhances the CNTFET's sensitivity, making it more responsive to small changes in gate voltage induced by the binding of SARS-CoV-2 antigens.

This behavior is attributed to larger diameter CNTs having a smaller bandgap, reducing the energy barrier for electron transport. Consequently, the device requires a lower voltage to turn on, which is beneficial for biosensing applications where detecting minute changes is essential. Optimizing the diameter of CNTs can significantly improve the performance of CNTFET-based biosensors in detecting SARS-CoV-2 [65].

Figure 11 depicts the gate voltage variation (V_g) with different concentrations of SARS-CoV-2. The graph shows a rapid increase in gate voltage with increasing virus concentration, which eventually levels off at higher concentrations. This saturation effect indicates that the binding sites on the CNTs are fully occupied at higher concentrations, leading to a steady-state gate voltage.

The initial rapid increase in V_g is due to the effective binding of SARS-CoV-2 antigens to the functionalized CNTs,

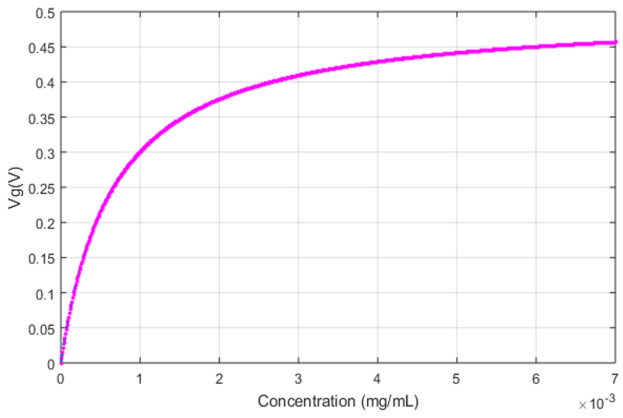

Figure 10. CNTFET threshold voltage as a function of diameter.

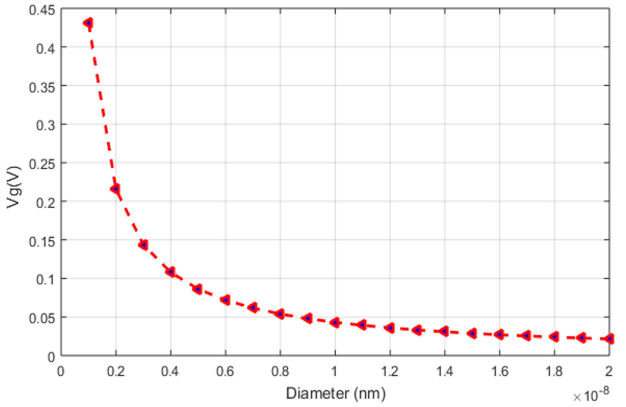

Figure 11. Gate voltage as a function of SARS-CoV-2 virus concentrations.

inducing a significant change in the electrical properties of the CNTFET. This relationship is critical for calibrating the sensor, ensuring that it provides accurate, real-time measurements of virus concentration in biological samples. The ability to detect varying concentrations of SARS-CoV-2 with high sensitivity is a crucial advantage of CNTFET-based biosensors [66].

Figure 12 illustrates the drain current (I_{ds}) versus drain voltage (V_{ds}) characteristics for different concentrations of SARS-CoV-2. The graph shows that higher virus concentrations result in increased drain current, reflecting the enhanced conductivity of the CNT channel due to the binding of negatively charged antigens. This increase in I_{ds} with higher concentrations demonstrates the sensor's ability to distinguish between different levels of viral load. The distinct separation of the curves for different concentrations confirms the high sensitivity and specificity of the CNTFET biosensor [67], which is crucial for practical applications, enabling quantitative analysis of SARS-CoV-2 in various samples.

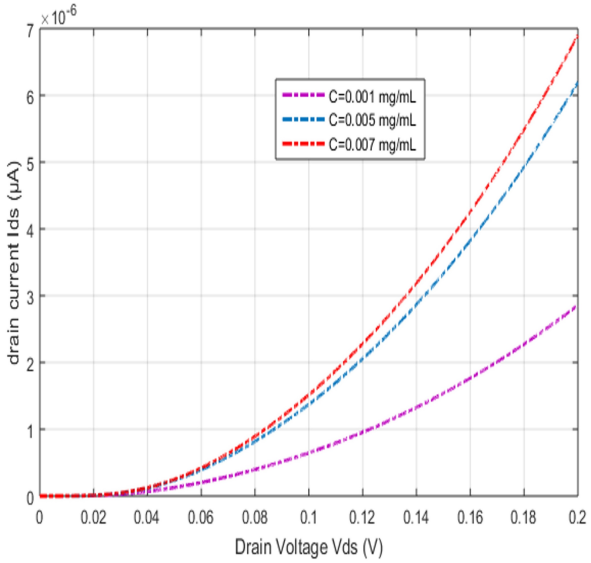

Figure 12. I_{ds} (V_{ds}) characteristic for different concentrations of SARS-CoV-2 virus.

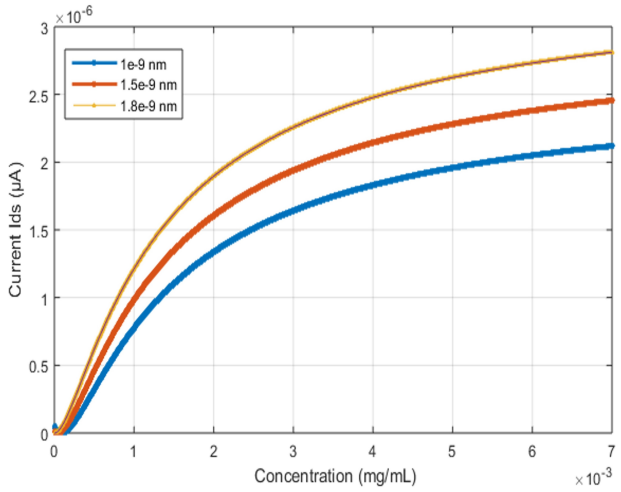

Figure 13. Drain current as a function of SARS-CoV-2 virus concentrations for different CNT diameters.

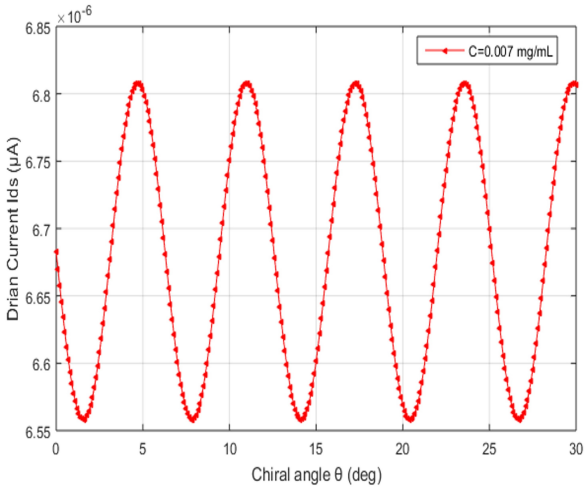

Figure 15. Drain current as a function of chirality angles.

Figure 13 shows the drain current (I_{ds}) as a function of SARS-CoV-2 virus concentrations for CNTs with different diameters (1.0 nm, 1.5 nm, and 1.8 nm). The graph indicates that larger diameters result in higher drain currents at the same virus concentration. This is because larger diameter CNTs have a greater surface area, facilitating more effective binding of SARS-CoV-2 antibodies and enhancing the overall conductivity of the CNTFET. This observation underscores the importance of selecting CNTs with optimal diameters to maximize biosensor sensitivity. By selecting CNTs with larger diameters, the biosensor can achieve higher currents for the same virus concentration, thereby improving the detection capability.

Figure 14 illustrates the relationship between drain current (I_{ds}) and SARS-CoV-2 virus concentrations for CNTs with different chirality angles. The graph shows that varying the chirality angle influences the drain current, although the overall effect is less pronounced than diameter variations.

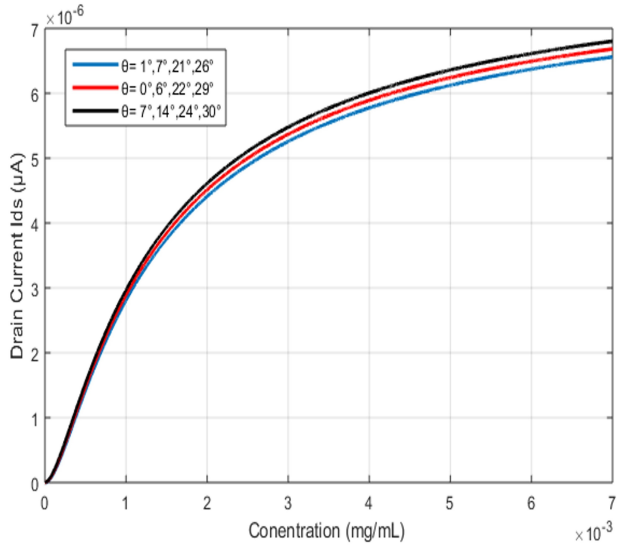

Figure 14. Drain current as a function of SARS-CoV-2 virus concentrations for different chirality angles.

The chirality angle determines whether a CNT behaves as a metallic or semiconducting material, affecting its electronic properties. CNTs with optimal chirality angles can exhibit enhanced electron transport properties, leading to higher sensitivity in detecting SARS-CoV-2 [68]. This observation underscores the need to optimize the chirality angle to improve sensor performance.

Figure 15 presents the drain current (I_{ds}) as a function of chirality angles for a fixed concentration of SARS-CoV-2 (0.007 mg/mL). The graph shows a periodic variation in drain current with changing chirality angles. The periodicity results from the inherent electronic properties of CNTs, which vary cyclically with the chirality angle. Understanding this periodic behavior is crucial for designing CNTFETs with specific electronic characteristics tailored for biosensing applications. By selecting CNTs with chirality angles that maximize drain current, the sensitivity of the biosensor can be significantly enhanced [69].

Figure 16 shows the drain current (I_{ds}) as a function of CNT length for a fixed concentration of SARS-CoV-2 (0.007 mg/mL). The graph indicates that the drain current initially

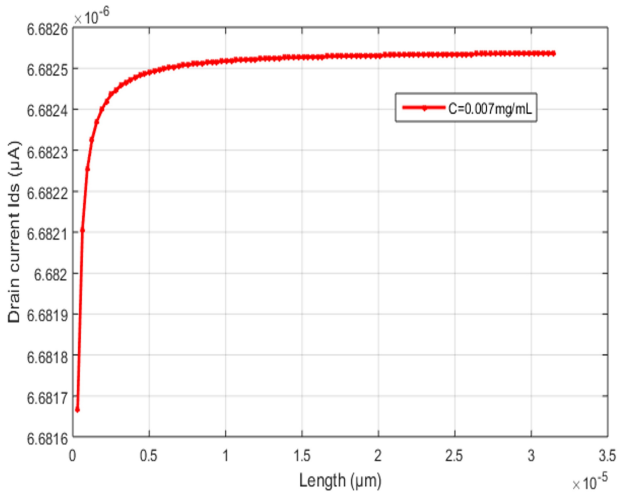

Figure 16. Drain current as a function of CNT length.

increases rapidly with length, then stabilizes as the length continues to increase. This behavior can be attributed to the ballistic transport of electrons within shorter CNTs, where resistance is minimal. As the length increases beyond the mean free path, resistance increases, and the current reaches a steady state. Optimizing the length of CNTs is essential to maintaining high sensitivity and low resistance in CNT-FET biosensors [70]. By selecting CNTs with appropriate lengths, the biosensor can achieve optimal performance by balancing sensitivity and resistance.

These results underscore the critical importance of optimizing CNT geometry and electronic properties to enhance the performance of CNTFET biosensors. By carefully tuning parameters such as diameter, chirality angle, and length, we can significantly improve the sensitivity and specificity of CNTFETs for SARS-CoV-2 detection. This optimization is essential for developing highly effective and reliable biosensors that can play a pivotal role in pandemic response efforts by enabling the rapid and accurate detection of viral infections.

5. Conclusion

The COVID-19 pandemic has underscored the urgent need for rapid, sensitive, and cost-effective diagnostic technologies, particularly in resource-limited settings. This study demonstrates the potential of carbon nanotube field-effect transistors (CNTFETs) as highly effective biosensors for SARS-CoV-2 detection. By leveraging the unique properties of carbon nanotubes, such as exceptional electrical conductivity and the ability to be functionalized with specific antibodies, we optimized key design parameters, including diameter, chirality angle, and length. The results show that optimized CNT geometries significantly enhance sensor performance, with smaller diameters, ideal chiral angles, and appropriate lengths providing high sensitivity to varying SARS-CoV-2 concentrations. These findings confirm the effectiveness of CNTFETs in viral detection and highlight their potential for broader diagnostic applications. Continued research should focus on refining these biosensors to enhance their role in global health preparedness and response to emerging threats.

Authors contributions
Oussama Zeggai: Conceptualization (lead); Software (lead); Writing – original draft (lead); Project administration (equal); Data curation (equal); Formal analysis (equal); Investigation (equal); Methodology (equal); Writing – review and editing (equal); Supervision (equal). Mousaab Belarbi: Conceptualization (equal); Project administration (lead); Data curation (equal); Formal analysis (equal); Investigation (lead); Methodology (equal); Software (equal); Writing – original draft (equal); Writing – review and editing (lead); Supervision (lead). Abdesslam Bouhenna: Methodology (supporting); Resources (equal); Visualization (equal). Sami Khettaf: Project administration (equal); Investigation (equal); Visualization (supporting). Hadj Mouloudj: Investigation (supporting); Resources (equal); Visualization (supporting). Amaria Ouledabbes: Resources (supporting); Visualization (supporting); Supervision (equal).

Availability of data and materials
The data supporting the findings of this study are available from the corresponding author upon reasonable request.

Conflict of interests
The authors declare that they have no known competing financial interests or personal relationships that could have appeared to influence the work reported in this paper.

References

[1] T. Acter, N. Uddin, J. Das, A. Akhter, T. Rabia Choudhury, and S. Kim. "Evolution of severe acute respiratory syndrome coronavirus 2 (SARS-CoV-2) as coronavirus disease 2019 pandemic COVID-19 : A global health emergency.". *Science of The Total Environment*, **730**:138996, 2020. DOI: https://doi.org/10.1016/j.scitotenv.2020.138996.

[2] M. Alafeef and D. Pan. "Diagnostic approaches for COVID-19: lessons learned and the path forward.". *ACS Nano.*, **16**:11545–11576, 2022. DOI: https://doi.org/10.1021/acsnano.2c01697.

[3] A. Afzal. "Molecular diagnostic technologies for COVID-19: Limitations and challenges.". *Journal of Advanced Research*, **26**:149–159,2090–1232, 2020. DOI: https://doi.org/10.1016/j.jare.2020.08.002.

[4] S. H. Safiabadi Tali, J. J. LeBlanc, Z. Sadiq, O. D. Oyewunmi, C. Camargo, B. Nikpour, N. Armanfard, S. M. Sagan, and S. Jahanshahi-Anbuh. "Tools and techniques for severe acute respiratory syndrome

coronavirus 2 (SARS-CoV-2)/COVID-19 detection. ". *Clinical Microbiology Reviews*, **34**, 2021. DOI: https://doi.org/10.1128/cmr.00228-20.

[5] G. Rahman, Z. Najaf, A. Mehmood, S. Bilal, A. ul Haq Ali Shah, S. Ahmad Mian, and G. Ali. "An Overview of the recent progress in the synthesis and applications of carbon nanotubes. ". *C — Journal of Carbon Research*, **5**:3, 2019. DOI: https://doi.org/10.3390/c5010003.

[6] A. Nehra and K. Pal Singh. "Current trends in nanomaterial embedded field effect transistor-based biosensor. ". *Biosensors and Bioelectronics*, **74**:731–743, 2015. DOI: https://doi.org/10.1016/j.bios.2015.07.030.

[7] N. Yang, X. Chen, T. Ren, P. Zhang, and D. Yang. "Carbon nanotube based biosensors. ". *Sensors and Actuators B: Chemical*, **207**:690–715, 2015. DOI: https://doi.org/10.1016/j.snb.2014.10.040.

[8] S. Gupta, C. N. Murthy, and C. Ratna Prabha. "Recent advances in carbon nanotube based electrochemical biosensors.". *International Journal of Biological Macromolecules*, **108**:687–703, 2018. DOI: https://doi.org/10.1016/j.ijbiomac.2017.12.038.

[9] T. T. Tran and A. Mulchandani. "Carbon nanotubes and graphene nano field-effect transistor-based biosensors. ". *TrAC Trends in Analytical Chemistry*, **79**:222–232, 2016. DOI: https://doi.org/10.1016/j.trac.2015.12.002.

[10] B. Dai, R. Zhou, J. Ping, Y. Ying, and L. Xie. "Recent advances in carbon nanotube-based biosensors for biomolecular detection. ". *TrAC Trends in Analytical Chemistry*, **154**:116658, 2022. DOI: https://doi.org/10.1016/j.trac.2022.116658.

[11] D. Sadighbayan, M. Hasanzadeh, and E. Ghafar-Zadeh. "Biosensing based on field-effect transistors (FET): recent progress and challenges ". *TrAC Trends in Analytical Chemistry*, **133**:116067, 2020. DOI: https://doi.org/10.1016/j.trac.2020.116067.

[12] G. Rabbani, M. Ehtisham Khan, E. Ahmad, M. Vahid Khan, A. Ahmad, A. Ulla Khan, W. Ali, M. A. Zamzami, A. H. Bashiri, and W. Zakri. "Serum CRP biomarker detection by using carbon nanotube field-effect transistor (CNT-FET) immunosensor.". *Bioelectrochemistry*, **153**:108493, 2023. DOI: https://doi.org/10.1016/j.bioelechem.2023.108493.

[13] G. Rabbani, M. Ehtisham Khan E. Ahmad, A. Ulla Khan, M. A. Zamzami, A. Ahmad, S. K. Ali, A. H. Bashiri, and W. Zakri. "Synthesis of carbon nanotubes-chitosan nanocomposite and immunosensor fabrication for myoglobin detection: an acute myocardial infarction biomarker. ". *International Journal of Biological Macromolecules*, **265**:130616, 2024. DOI: https://doi.org/10.1016/j.ijbiomac.2024.130616.

[14] W. Reis de Araujo, H. Lukas, M. D. T. Torres, W. Gao, and C. de la Fuente-Nunez. "Low-Cost biosensor technologies for rapid detection of COVID-19 and future pandemics". *ACS Nano*, **18**:1757–1777, 2024. DOI: https://doi.org/10.1021/acsnano.3c01629.

[15] R. Wang, S. Lu, F. Deng, L. Wu, G. Yang, S. Chong, and Y. Liu. "Enhancing the understanding of SARS-CoV-2 protein with structure and detection methods: an integrative review.". *International Journal of Biological Macromolecules*, **270**:132237, 2024. DOI: https://doi.org/10.1016/j.ijbiomac.2024.132237.

[16] Y. Liang, M. Xiao, J. Xie, J. Li, Y. Zhang, H. Liu, Y. Zhang, J. He, G. Zhang, N. Wei, L. M. Peng, Y. Ke, and Z. Y. Zhang. "Amplification-free detection of SARS-CoV-2 down to single virus level by portable carbon nanotube biosensors. ". *Small*, **19**:2208198, 2023. DOI: https://doi.org/10.1002/smll.202208198.

[17] F. Mirzadeh-rafie, F. Rahbarizadeh, N. Shoaei, F. Nasiri, M. R. Akbarizadeh, and M. Khatami. "Carbon nanoparticle-based COVID-19 biosensors. ". *Sensors International*, **4**:100246, 2023. DOI: https://doi.org/10.1016/j.sintl.2023.100246.

[18] M. Thanihaichelvan, S. N. Surendran, T. Kumanan, U. Sutharsini, P. Ravirajan, R. Valluvan, and T. Tharsika. "Selective and electronic detection of COVID-19 (Coronavirus) using carbon nanotube field effect transistor-based biosensor: A proof-of-concept study. ". *Materials Today: Proceedings*, **49**:2546–2549, 2022. DOI: https://doi.org/10.1016/j.matpr.2021.05.011.

[19] H. A. Rothan and S. N. Byrareddy. "The epidemiology and pathogenesis of coronavirus disease (COVID-19) outbreak.". *Journal of Autoimmunity*, **109**:102433, 2020. DOI: https://doi.org/10.1016/j.jaut.2020.102433.

[20] S. Ludwig and Z. Alexander. "Coronaviruses and SARS-CoV-2: a brief overview.". *Anesthesia & Analgesia*, **131**:93–96, 2020. DOI: https://doi.org/10.1213/ANE.0000000000004845.

[21] S. Su, G. Wong, W. Shi, J. Liu, A. C. K. Lai, J. Zhou, W. Liu, Y. Bi, and G. F. Gao. "Epidemiology, genetic recombination, and pathogenesis of coronaviruses. ". *Trends Microbiology*, **24**:490–502, 2016. DOI: https://doi.org/10.1016/j.tim.2016.03.003.

[22] J. Cui, F. Li, and Z. L. Shi. "Origin and evolution of pathogenic coronaviruses.". *Nature Reviews Microbiology*, **17**:181–192, 2019. DOI: https://doi.org/10.1038/s41579-018-0118-9.

[23] C. I. Paules, H. D. Marston, and A. S. Fauci. "Coronavirus infections—more than just the common cold.". *JAMA*, **323**:707–708, 2020. DOI: https://doi.org/10.1001/jama.2020.0757.

[24] M. A. Shereen, S. Khan, A. Kazmi, N. Bashir, and R. Siddique. "COVID-19 infection: origin, transmission, and characteristics of human coronaviruses. ". *Journal of Advanced Research*, **24**:91–98, 2020. DOI: https://doi.org/10.1016/j.jare.2020.03.005.

[25] L. Meng, F. Hua, and Z. Bian. "Coronavirus disease 2019 (COVID-19): emerging and future challenges for dental and oral medicine.". *Journal of Dental Research*, **99**:481–487, 2020. DOI: https://doi.org/10.1177/0022034520914246.

[26] G. Rabbani, S. Nate Ahn, H. Kwon, K. Ahmad, and I. Choi. "Penta-peptide ATN-161 based neutralization mechanism of SARS-CoV-2 spike protein. ". *Biochemistry and Biophysics Reports*, **28**:101170, 2021. DOI: https://doi.org/10.1016/j.bbrep.2021.101170.

[27] G. Rabbani and S. Nate Ahn. "Review: Roles of human serum albumin in prediction, diagnoses and treatment of COVID-19. ". *International Journal of Biological Macromolecules*, **193**:948–955, 2021. DOI: https://doi.org/10.1016/j.ijbiomac.2021.10.095.

[28] N. Khadijeh, M. Parham, K. Ehsaneh, E. Zeinalzadeh, G. Khudaverdi, Asgharzadeh, and K. H. Samadi. "SARS-CoV-2 receptor ACE2 and molecular pathway to enter target cells during infection.". *Reviews and Research in Medical Microbiology*, **33**:105–113, 2022. DOI: https://doi.org/10.1097/MRM.0000000000000237.

[29] A. J. Saleh Ahammad, J. J. Lee, and Md. Aminur Rahman. "Electrochemical sensors based on carbon nanotubes. ". *Sensors*, **9**:2289–2319, 2009. DOI: https://doi.org/10.3390/s90402289.

[30] J. Wang. "Carbon-nanotube based electrochemical biosensors: a review. ". *Electroanalysis*, **17**:7–14, 2005. DOI: https://doi.org/10.1002/elan.200403113.

[31] T. G. Cha, B. A. Baker, M. D. Sauffer, J. Salgado, D. Jaroch, J. L. Rickus, D. M. Porterfield, and J. H. Choi. "Optical nanosensors architecture for cell-signaling molecules using DNA aptamer-coated carbon nanotubes.". *ACS Nano*, **5**:4236–4244, 2011. DOI: https://doi.org/10.1021/nn201323h.

[32] N. M. Bandaru and N. H. Voelcker. "Glycoconjugate-functionalized carbon nanotubes in biomedicine.". *Journal of Materials Chemistry*, **22**:8748–8758, 2012. DOI: https://doi.org/10.1039/C2JM16636D.

[33] X. N. Wang and P. A. Hu. "Carbon nanomaterials: Controlled growth and field-effect transistor biosensors.". *Frontiers of Materials Science*, **6**:26–46, 2012. DOI: https://doi.org/10.1007/s11706-012-0160-x.

[34] R. S. Park, G. Hills, J. Sohn, S. Mitra, M. M. Shulaker, and H.-S. Philip Wong. "Hysteresis-free carbon nanotube field-effect transistors. ". *ACS Nano*, **11**:4785–4791, 2017. DOI: https://doi.org/10.1021/acsnano.7b01164.

[35] Y. Lin, S. Taylor, H. Li, K. A. Fernando, L. Qu, W. Wang, L. Gu, B. Zhou, and Y. P. Sun. "Advances toward bioapplications of carbon nanotubes. ". *Journal of Materials Chemistry*, **14**:527–541, 2004. DOI: https://doi.org/10.1039/B314481J.

[36] M. Kalbacova, M. Kalba, L. Dunsch, H. Kataura, and U. Hempel. "The study of the interaction of human mesenchymal stem cells and monocytes/macrophages with single-walled carbon nanotube films. ". *Physica Status Solidi B*, **243**:3514–3518, 2006. DOI: https://doi.org/10.1002/pssb.200669167.

[37] V. N. Popov. "Carbon nanotubes: properties and application. ". *Materials Science and Engineering: R: Reports*, **43**:61–102, 2004. DOI: https://doi.org/10.1016/j.mser.2003.10.001.

[38] D. C. Ferrier and K. C. Honeychurch. "Carbon nanotube (CNT)-based biosensors.". *Biosensors*, **11**:1–34, 2021. DOI: https://doi.org/10.3390/bios11120486.

[39] D. G. Agh Kaariz, E. Darabi, and S. M. Elahi. "Fabrication of Au/ZnO/MWCNTs electrode and its characterization for electrochemical cholesterol biosensor.". *Journal of Theoretical and Applied Physics (JTAP)*, **14**:1, 2020. DOI: https://doi.org/10.1007/s40094-020-00390-5.

[40] M. Terrones. "Science and technology of the twenty-first century: synthesis, properties, and applications of carbon nanotubes. ". *Annual Review of Materials Research*, **33**:419–50, 2003. DOI: https://doi.org/10.1146/annurev.matsci.33.012802.100255.

[41] R. Saito, G. Dresselhaus, and M. S. Dresselhaus. "Physical properties of carbon nanotubes. ". *World Scientific*, **4**:272, 1998. DOI: https://doi.org/10.1142/p080.

[42] A. Mouatsi and M. Marir-Benabbas. "Modeling of sub-band and diameter effect in carrier concentration of CNTFET.". *Materials Science in Semiconductor Processing*, **28**:115–120, 2014. DOI: https://doi.org/10.1016/j.mssp.2014.07.033.

[43] P. S. Raja, R. J. Daniel, and N. Bino. "Performance analysis of carbon nano tubes.". *Journal of Engineering (IOSRJEN)*, **2**:54–58, 2012. DOI: https://doi.org/10.9790/3021-02815458.

[44] K. M. Sundaram, P. Prakash, D. Karthikeyan, and W. D. Mammo. "Improved carbon nanotube field effect transistor for designing a hearing aid filtering application. ". *Journal of Nanomaterials*, :1–12, 2021. DOI: https://doi.org/10.1155/2021/7024032.

[45] S. Yamacli and M. Avci. "Accurate SPICE compatible CNT interconnect and CNTFET models for circuit design and simulation. ". *Mathematical and Computer Modelling*, **58**:368–378, 2013. DOI: https://doi.org/10.1016/j.mcm.2012.11.014.

[46] Y. Liu, M. S. Moura, A. J. Costa, L. A. L de Almeida, M. Paranjape, and M. Fontana. "Modeling in ballistic carbon nanotube field-effect transistors. ". *Nanotechnology, Science and Applications*, **7**:55–61, 2014. DOI: https://doi.org/10.2147/NSA.S58003.

[47] A. Saberkari, O. Khorgami, J. Bagheri, M. Madec, S. M. Hosseini-Golgoo, and E. Alarcón-Cot. "Design of broadband CNFET LNA based on extracted I-V closed-form equation. ". *IEEE Transactions on Nanotechnology*, **17**:731–742, 2018. DOI: https://doi.org/10.1109/TNANO.2018.2822599.

[48] A. N. Kozitsina, T. S. Svalova, N. N. Malysheva, A. V. Okhokhonin, M. B. Vidrevich, and K. Z. Brainina. "Sensors based on bio and biomimetic receptors in medical diagnostic, environment, and food analysis.". *Biosensors*, **8**:1–35, 2018. DOI: https://doi.org/10.3390/bios8020035.

[49] O. Zeggai, A. Ouldabbas, M. Bouchaour, and H. Zeggai. "Biological detection by high electron mobility transistor (HEMT) based AlGaN/GaN. ". *Physica Status Solidi C*, **11**:274–279, 2014. DOI: https://doi.org/10.1002/PSSC.201300296.

[50] O. Zeggai, M. Belarbi, A. Ouledabbes, and H. Mouloudj. "Modeling of a micro-biological sensor field effect for the enzymatic detection of glucose. ". *International Journal of Modern Physics B*, **33**:19502898, 2019. DOI: https://doi.org/10.1142/S0217979219502898.

[51] G. Lu, L. E. Ocola, and J. Chen. "Reduced graphene oxide for room-temperature gas sensors.". *Nanotechnology*, **20**:1–9, 2009. DOI: https://doi.org/10.1088/0957-4484/20/44/445502.

[52] S. Cui, H. Pu, S. A. Wells, Z. Wen, S. Mao, J. Chang, M. C. Hersam, and J. Chen. "Ultrahigh sensitivity and layer-dependent sensing performance of phosphorene-based gas sensors.". *Nature Communications*, **6**:8632, 2015. DOI: https://doi.org/10.1038/ncomms9632.

[53] G. Zhou, J. Chang, S. Cui, H. Pu, Z. Wen, and J. Chen. "Real-time, selective detection of Pb^{2+} in water using a reduced graphene oxide/gold nanoparticle field-efect transistor device.". *ACS Applied Materials and Interfaces*, **6**:19235–19241, 2014. DOI: https://doi.org/10.1021/am505275a.

[54] K. Chen, G. Lu, J. Chang, S. Mao, K. Yu, S. Cui, and J. Chen. "Hg(II) Ion detection using thermally reduced graphene oxide decorated with functionalized gold nanoparticles. ". *Analytical Chemistry*, **84**:4057–4062, 2012. DOI: https://doi.org/10.1021/ac3000336.

[55] J. Kim, S. Jeong, S. Sarawut, H. Kim, S. Uk Son, S. Lee, G. Rabbani, H. Kwon, E. K. Lim, S. Nate Ahn, and S. H. K. Park. "An immunosensor based on a high performance dual-gate oxide semiconductor thin-film transistor for rapid detection of SARS-CoV-2. ". *Lab Chip*, **22**:899–907, 2022. DOI: https://doi.org/10.1039/D1LC01116B.

[56] S. Mao, Ke. Yu, J. C., D. A. Steeber, L. E. Ocola, and J. Chen. "Direct growth of vertically-oriented graphene for feld-efect transistor biosensor. ". *Scientific Reports*, **3**:1696, 2013. DOI: https://doi.org/10.1038/srep01696.

[57] S. Mao, G. Lu, K. Yu, Z. Bo, and J. Chen. "Specifc protein detection using termally reduced graphene oxide sheet decorated with gold nanoparticle-antibody conjugates.". *Advanced Materials*, **22**:3521–3526, 2010. DOI: https://doi.org/10.1002/adma.201000520.

[58] H. Meskher, H. C. Mustansar, A. K. Thakur, R. Sathyamurthy, I. Lynch, P. Singh, T. K. Han, and R. Saidur. "Recent trends in carbon nanotube (CNT)-based biosensors for the fast and sensitive detection of human viruses: a critical review.". *Nanoscale Advances*, **5**:992–1010, 2023. DOI: https://doi.org/10.1039/D2NA00236A.

[59] M. A. Zamzami, G. Rabbani, A. Ahmad, A. A. Basalah, W. H. Al-Sabban, S. Nate Ahn, and H. Choudhry. "Carbon nanotube field-effect transistor (CNT-FET)-based biosensor for rapid detection of SARS-CoV-2 (COVID-19) surface spike protein S1. ". *Bioelectrochemistry*, **143**:107982, 2022. DOI: https://doi.org/10.1016/j.bioelechem.2021.107982.

[60] R. L. Pinals, F. Ledesma, D. Yang, N. Navarro, S. Jeong, J. E. Pak, L. Kuo, Y. C. Chuang, Y. W. Cheng, H. Y. Sun, and M. P. Landry. "Rapid SARS-CoV-2 spike protein detection by carbon nanotube-based near-infrared nanosensors. ". *Nano letters*, **21**:2272–2280, 2021. DOI: https://doi.org/10.1021/acs.nanolett.1c00118.

[61] G. Seo, G. Lee, M. J. Kim, S. H. Baek, M. Choi, K. Bon Ku, C. S. Lee, S. Jun, D. Park, H. Gi Kim, S. J. Kim, J. O Lee, B. Tae Kim, E. C. Park, and S. I. Kim. "Rapid detection of COVID-19 causative virus (SARS-CoV-2) in human nasopharyngeal swab specimens using field-effect transistor-based biosensor.". *ACS Nano*, **14**:5135–5142, 2020. DOI: https://doi.org/10.1021/acsnano.0c02823.

[62] W. Shao, M. R. Shurin, S. E. Wheeler, X. He, and A. Star. "Rapid detection of SARS-CoV-2 antigens using high-purity semiconducting single-walled carbon nanotube-based field effect transistors.". *ACS Applied Materials and Interfaces*, **13**:10321–10327, 2021. DOI: https://doi.org/10.1021/acsami.0c22589.

[63] B. Ghosh and A. Gramin. "First principle study of the effect of defects on performance of single-molecule pentacene field effect transistors.". *Journal of Theoretical and Applied Physics (JTAP)*, **9**:213–219, 2015. DOI: https://doi.org/10.1007/s40094-015-0182-8.

[64] M. Xian, H. Luo, X. Xia, C. Fares, P. H. Carey, C. W. Chiu, F. Ren, S. S. Shan, Y. T. Liao, S. M. Hsu, J. F. Esquivel-Upshaw, C. W. Chang, J. Lin, Steven C. Ghivizzani, and S. J. Pearton. "Fast SARS-CoV-2 virus detection using disposable cartridge strips and a semiconductor-based biosensor platform. ". *Journal of Vacuum Science and Technology B*, **39**:1–7, 2021. DOI: https://doi.org/10.1116/6.0001060.

[65] F. Zahoor, M. Hanif, U. I. Bature, S. Bodapati, A. Chattopadhyay, F. Azmadi Hussin, H. Abbas, F. Merchant, and F. Bashir. "Carbon nanotube field effect transistors: an overview of device structure, modeling, fabrication and applications. ". *Physica Scripta*, **98**: 082003, 2023. DOI: https://doi.org/10.1088/1402-4896/ace855.

[66] E. N. Özmen, E. Kartal, M. B. Turan, A. Yazıcıoğlu, J. H. Niazi, and A. Qureshi. "Graphene and carbon nanotubes interfaced electrochemical nanobiosensors for the detection of SARS-CoV-2 (COVID-19) and other respiratory viral infections: a review. ". *Materials Science and Engineering: C*, **129**:112356, 2021. DOI: https://doi.org/10.1016/j.msec.2021.112356.

[67] S. Mukherjee, D. Bandyopadhyay, P. Kishore Dutta, and S. Kumar Sarkar. "Quantum analytical modeling and simulation of CNT on insulator (COI) and CNT on nothing (CON) FET: a comparative analysis. ". *Journal of Theoretical and Applied Physics (JTAP)*, **10**:91–97, 2016. DOI: https://doi.org/10.1007/s40094-015-0205-5.

[68] P. Liu, Y. Jiao, X. Chai, Y. Ma, S. Liu, X. Fang, F. Fan, L. Xue, J. Han, and Q. Liu. "High-performance electric and optical biosensors based on single-walled carbon nanotubes.". *Journal of Luminescence*, **250**:119084, 2022. DOI: https://doi.org/10.1016/j.jlumin.2022.119084.

[69] J. M. Park and S. N. Hong. "Efficient compact model for calculating the surface potential of carbon-nanotube field-effect transistors using a curve-fitting method. ". *Current Applied Physics*, **15**:938–942, 2015. DOI: https://doi.org/10.1016/j.cap.2015.05.002.

[70] M. Thanihaichelvan. "Carbon nanotube and graphene field-effect transistors for aptamer and odorant receptor-based biosensors. ". *Te Herenga Waka-Victoria University of Wellington (Thesis)*, , 2019. DOI: https://doi.org/10.26686/wgtn.22783295.